

# Modeling and variable structure power control of PMSG based variable speed wind energy conversion system

Y. ERRAMI<sup>a</sup>, M. OUASSAID<sup>b</sup>, M. MAAROUFI<sup>a</sup>

<sup>a</sup>Department of Electrical Engineering, Ecole Mohammadia d'Ingénieurs-University Mohammed V Agdal, Rabat-Morocco

<sup>b</sup>Departement of Industrial Engineering, National School of Application Sciences (ENSA-Safi), Cadi Ayyad University, Safi, Morocco

In the proposed Wind Energy Conversion System (WECS) a Permanent Magnet Synchronous Generator (PMSG) is used as a variable speed generator. The WECS model includes a wind turbine, a PMSG, PWM rectifier in generator-side, intermediate DC circuit and PWM inverter in grid-side. In this work, the control strategy combines Sliding Mode (SM) nonlinear control and Maximum Power Point Tracking (MPPT) control strategy to maximize the generated power from Wind Turbine Generator (WTG). Besides, considering the variation of wind speed, both converters use the SM scheme. The PMSG side converter is used to achieve MPPT, while the grid-side converter regulates DC-link voltage and injects the generated power into the AC network. Active and reactive power are controlled by direct and quadrature current components, respectively. On the other hand, the pitch angle is active in high wind speeds and it is designed to prevent WTG damage from excessive wind speed. Furthermore, the results of the simulation are shown to verify the effectiveness and to prove the concept of the control strategy.

(Received September 28, 2013; accepted November 7, 2013)

**Keywords:** WECS, PMSG, MPPT, Lyapunov theory, Sliding Mode control, Unity power factor

## 1. Introduction

In recent years, there has been a developing interest in wind energy as it is a potential source for electricity generation with minimal environmental impact [1-2]. The wind generation systems are getting a lot of attention, because their costs are competitive, environmentally clean and safe renewable power sources, if we compare them to fossil fuel and nuclear power generation [2]. At present, the variable generation system is becoming the most important and fastest growing application of wind generation system [3-4]. On the other hand, there are mainly three types of generators which are used in wind power system: Induction Generator (IG), Doubly Fed Induction Generator (DFIG) and Permanent Magnet Synchronous Generator (PMSG) [5-8]. PMSG is an attractive choice for variable-speed generation system. It is connected directly to the turbine without gearbox and does not require any external excitation current. So it can operate at low speeds and reduce again weight, losses, costs and maintenance requirements [9-13].

This paper proposes a control strategy of direct-drive permanent magnet wind power system, and discusses back-to-back PWM converter control method. We present a complete detailed modeling and a control scheme of a three-phase grid-connected WECS. The control algorithm incorporates a MPPT. The WECS model includes a wind turbine, a PMSG, PWM rectifier in generator-side, intermediate DC circuit, and PWM inverter in grid-side. PMSG is coupled to wind turbine without gearbox. The speed of PMSG is suitably controlled according to a wind

velocity and thus the power from a wind turbine settles down on the maximum power point by the proposed MPPT control. The speed control is realized through SM nonlinear control where the q-axis current is used to control the rotational speed of the generator according to the variation of wind speed and the d-axis current is set to zero. The controller is designed through the Lyapunov stable theory to ensure the stability of the controller and achieve the required control result. As the voltage and frequency of generator output vary along the wind speed change, the generator-side converter is used to track the maximum wind power and implement Sliding Mode control for PMSG. Inverter is used to sustain the DC-bus voltage and regulate the grid-side power factor. Thus, active and reactive powers are controlled respectively by the inverter in grid-side [9].

This paper is structured as follows. In Sections 2 the models of the wind turbine generator and PMSG are developed. In Section 3, control of system will be presented. The simulations results are given in Section 4. Finally, some conclusions are presented in Section 5.

## 2. Mathematical Modeling of WECS

### 2.1 Model of wind turbine with PMSG

Wind turbine can not fully capture wind energy. So, output aerodynamic power of the wind-turbine is expressed as [3]:

$$P_{Turbine} = \frac{1}{2} \rho A C_p(\lambda, \beta) v^3 \quad (1)$$

where,  $\rho$  is the air density (typically  $1.225 \text{ kg/m}^3$ ),  $A$  is the area swept by the rotor blades (in  $\text{m}^2$ ),  $C_p$  is the coefficient of power conversion and  $v$  is the wind speed (in  $\text{m/s}$ ).

The tip-speed ratio is defined as:

$$\lambda = \frac{\omega_m R}{v} \quad (2)$$

where  $\omega_m$  and  $R$  are the rotor angular velocity (in  $\text{rad/sec}$ ) and rotor radius (in  $\text{m}$ ), respectively.

The wind turbine mechanical torque output  $T_m$  given as:

$$T_m = \frac{1}{2} \rho A C_p(\lambda, \beta) v^3 \frac{1}{\omega_m} \quad (3)$$

The power coefficient is a nonlinear function of the tip-speed ratio  $\lambda$  and the blade pitch angle  $\beta$  (in degrees). If the swept area of the blade and the air density are constant, the value of  $C_p$  is a function of  $\lambda$  and it is maximum at the particular  $\lambda_{opt}$ . Hence, to fully utilize the wind energy,  $\lambda$  should be maintained at  $\lambda_{opt}$ , which is determined from the blade design. Then:

$$P_{Turbine} = \frac{1}{2} \rho A C_{P_{max}} v^3 \quad (4)$$

A generic equation is used to model the power coefficient  $C_p(\lambda, \beta)$  based on the modeling turbine characteristics described in [5] as:

$$C_p = \frac{1}{2} \left( \frac{116}{\lambda_i} - 0.4\beta - 5 \right) e^{-\left(\frac{21}{\lambda_i}\right)} \quad (5)$$

$$\frac{1}{\lambda_i} = \frac{1}{\lambda + 0.08\beta} - \frac{0.035}{\beta^3 + 1}$$

The particular value  $\lambda_{opt}$  results in the point of optimal efficiency where the maximum power is captured from wind by the wind turbine. For each wind speed, there exists a specific point in the wind generator power characteristic, MPPT, where the output power is maximized. Thus, the control of the WECS load results in a variable-speed operation of the turbine rotor and the maximum power is extracted continuously from the wind (MPPT control) [10-11]. This is illustrated in Fig.1.

## 2.2 PMSG model

Dynamic modelling of PMSG can be described in d-q reference system as follows [3]:

$$v_{gd} = (R_g + pL_d) i_d - \omega_e L_q i_q \quad (6)$$

$$v_{gq} = (R_g + pL_q) i_q + \omega_e L_d i_d + \omega_e \psi_f \quad (7)$$

where  $R_g$  is the stator resistance,  $L_q$  and  $L_d$  are the inductances of the generator on the  $d$  and  $q$  axis,  $\psi_f$  is the permanent magnetic flux and  $\omega_e$  is the electrical rotating speed of the generator, defined by

$$\omega_e = p_n \omega_m \quad (8)$$

where  $p_n$  is the number of pole pairs of the generator and  $\omega_m$  is the mechanical angular speed. The expression for the electromagnetic torque can be described as:

$$T_e = \frac{3}{2} p_n \left[ \psi_f i_q - (L_d - L_q) i_d i_q \right] \quad (9)$$

If  $i_d = 0$ , the electromagnetic torque is expressed as:

$$T_e = \frac{3}{2} p_n \psi_f i_q \quad (10)$$

The dynamic equation of the wind turbine is given as:

$$J \frac{d\omega_m}{dt} = T_e - T_m - F \omega_m \quad (11)$$

where  $J$  is the total inertia,  $F$  is the viscous friction coefficient and  $T_m$  is the mechanical torque developed by the turbine.

## 3. Control of System

### 3.1 MPPT and Pitch control algorithms

For a given wind speed, the optimal rotational speed of the wind turbine rotor can be simply estimated as follows [6]:

$$\omega_{m-opt} = \frac{v \lambda_{opt}}{R} \quad (12)$$

The wind turbine can produce maximum power by (4). Then the maximum mechanical output power of the turbine is given as follows:

$$P_{Turbine} = \frac{1}{2} \rho A C_{P_{max}} \left( \frac{R \omega_{m-opt}}{\lambda_{opt}} \right)^3 \quad (13)$$

Then, we can get the maximum power  $P_{Turbine\_max}$  by regulating the turbine speed in different wind speed under rated power of the wind power system. Therefore, an optimum value of tip speed ratio  $\lambda_{opt}$  can be maintained

and maximum wind power can be captured. When the wind velocities are higher than rated, the maximum energy captured must be limited using pitch control by modifying  $\beta$ . The pitch angle will increase until the machine is at the rated speed. The relationship between the generator speed and the blade pitch angle  $\beta$  is illustrated in Fig.2 where  $P_g$  is the generated power. Thus, when the power output becomes too high the blade pitch is asked immediately to turn the blades slightly out of the wind. In addition, the rated rotor speed and the power are maintained for above rated wind speeds.

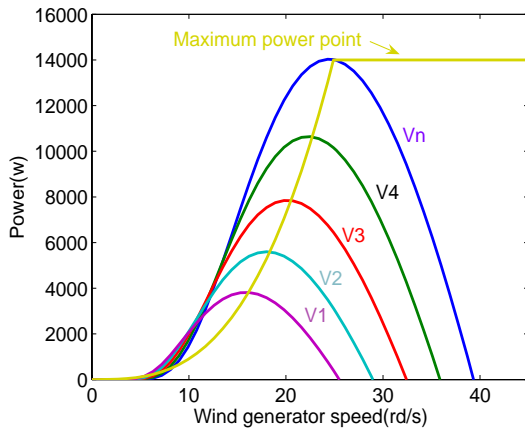


Fig.1. Wind generator power curves at various wind speed

### 3.2 Control of generator side converter with MPPT and sliding mode control

The generator side three-phase converter, which is used as a rectifier, uses a sliding mode control strategy and works as a driver controlling the generator operating at optimum rotor speed  $\omega_{m-opt}$  to obtain maximum energy from wind.

It is deduced from equations (10) and (11) that the wind turbine speed can be controlled by regulating the q-axis stator current components ( $i_{qr}$ ). The control objective is to track the rotor angular speed. In order to satisfy the sliding mode condition, we can define the sliding surface for the speed controller [14]:

$$S_{\omega} = \omega_{m-opt} - \omega_m \quad (14)$$

$\omega_{m-opt}$  is generated by a MPPT method. To determine the stabilizing function, the following Lyapunov function is defined as:

$$Y_{\omega} = \frac{1}{2} S_{\omega}^2 \quad (15)$$

Because the system stability needs to be proved, Lyapunov's stability theory is deployed. The following condition must be fulfilled:  $\frac{dY_{\omega}}{dt} = S_{\omega} \frac{dS_{\omega}}{dt} < 0$

When the sliding mode occurs on the sliding surface, then

$$S_{\omega} = \frac{dS_{\omega}}{dt} = 0.$$

So, currents references are derived to ensure the PMSG speed convergence to the optimum speed:

$$i_{dr} = 0 \quad (16)$$

$$i_{qr} = \frac{2}{3 p_n \psi_f} (T_m + J \frac{d\omega_{m-opt}}{dt} + F \omega_m + k_{\omega} \text{sgn}(S_{\omega})) \quad (17)$$

In order to regulate the currents to their references, a sliding mode control is used. Let us introduce the following sliding surfaces:

$$S(i_d) = i_{dr} - i_d \quad (18)$$

$$S(i_q) = i_{qr} - i_q \quad (19)$$

where  $i_{dr}$ ,  $i_{qr}$  are the desired values of d-axis current and q-axis current respectively. Then:

$$\frac{dS(i_d)}{dt} = \frac{di_{dr}}{dt} - \frac{di_d}{dt} \quad (20)$$

$$\frac{dS(i_q)}{dt} = \frac{di_{qr}}{dt} - \frac{di_q}{dt} \quad (21)$$

It is necessary to design the Lyapunov function to determine the required condition for the existence of the sliding mode. The function of Lyapunov is chosen as

$$Y = \frac{1}{2} S^2 \quad (22)$$

from Lyapunov's stability theory, in order to make the system stable [15],  $Y$  can be derived as,

$$\frac{dY}{dt} = S \frac{dS}{dt} < 0 \quad (23)$$

Combing (20), (21) and (23), that is

$$S(i_d) \frac{dS(i_d)}{dt} < 0 \quad (24)$$

$$S(i_q) \frac{dS(i_q)}{dt} < 0 \quad (25)$$

In order to obtain a good commutation around the surface and dynamic performances, the control includes two terms [15]:

$$u_c = u_{eq} + u_n \quad (26)$$

$u_{eq}$  is valid only in the sliding surface. In permanent regime and during the sliding mode,  $u_{eq}$  is calculated from the expression:

$$\dot{S}(x) = 0 \tag{27}$$

$x$  is  $i_d$  or  $i_q$ .  $u_n$  is used in order to guarantee the attractiveness of the variable to be controlled towards the commutation surface. Then

$$u_n = k_i \operatorname{sgn}(S(x)) \tag{28}$$

$i$  is  $d$  or  $q$  and  $k_i > 0$ .

Sliding mode is a discontinuous control. Therefore, to reduce the chattering, the continuous function as shown in (29) where  $\operatorname{sgn}(S(x))$  is a sign function defined as [16]:

$$\operatorname{sgn}(S(x)) = \begin{cases} 1 & S(x) > \varepsilon \\ \frac{S(x)}{\varepsilon} & \varepsilon \geq |S(x)| \\ -1 & -\varepsilon > S(x) \end{cases} \tag{29}$$

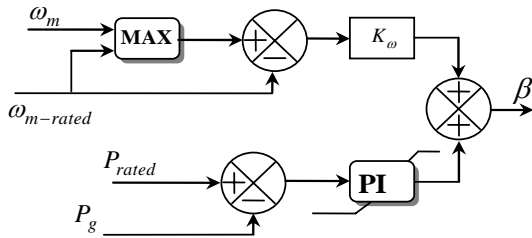


Fig.2. WECS pitch angle controller.

where  $\varepsilon$  is a small positive number. The dynamic quality of the system will be reduced if the  $\varepsilon$  is too small or too large. Then, the value of  $\varepsilon$  should be chosen carefully.

Thus, the controls voltage of d axis and q axis are defined by:

$$v_{dr} = R_g i_d - L_d \omega_e i_q + k_d \operatorname{sgn}(S(i_d)) \tag{30}$$

$$v_{qr} = R_g i_q + L_d \omega_e i_d + \omega_e \psi_f + L_q \frac{di_{qr}}{dt} + k_q \operatorname{sgn}(S(i_q)) \tag{31}$$

Finally, PWM is used to produce the control signal to implement the nonlinear control for the generator. The double closed-loop control diagram for generator-side converter is shown as Fig.3.

### 3.3 Control of load side inverter

The grid side three-phase converter feeds the generated energy into the grid, keeps the DC-link voltage constant and adjusts the amount of the active and reactive powers delivered to the grid during load transients or wind speed variations [5-6].

The SM controllers are used in order to regulate the output voltage, currents in the inner control loops and the DC voltage controller in the second loop (Fig.3).

The voltage balance across the inductor  $L_f$  is given by:

$$v_d = e_d - R_f i_{d-f} - L_f \frac{di_{d-f}}{dt} + \omega L_f i_{q-f} \tag{32}$$

$$v_q = e_q - R_f i_{q-f} - L_f \frac{di_{q-f}}{dt} - \omega L_f i_{d-f} \tag{33}$$

$$C \frac{dU_{dc}}{dt} = \frac{3}{2} \left( \frac{v_d}{U_{dc}} i_{d-f} + \frac{v_q}{U_{dc}} i_{q-f} \right) - i_{dc} \tag{34}$$

where  $L_f$  and  $R_f$  are the filter inductance and resistance respectively;  $e_d$  and  $e_q$  are the inverter d-axis q-axis voltage components respectively,  $v_d$  and  $v_q$  are the grid voltage components in the d-axis q-axis voltage components respectively;  $i_{d-f}$ ,  $i_{q-f}$  are the values of d-axis current and q- axis current respectively.  $U_{dc}$  is the DC-bus voltage,  $i_{dc}$  is the DC-bus current.

If the grid voltage space vector  $\vec{u}$  is oriented on d-axis, then:

$$\begin{aligned} v_d &= V \\ v_q &= 0 \end{aligned} \tag{35}$$

The voltage balance across the inductor  $L_f$  is given by:

$$\frac{di_{d-f}}{dt} = \frac{1}{L_f} (e_d - R_f i_{d-f} + \omega L_f i_{q-f} - V) \tag{36}$$

$$\frac{di_{q-f}}{dt} = \frac{1}{L_f} (e_q - R_f i_{q-f} - \omega L_f i_{d-f}) \tag{37}$$

Then the reactive power and active power can be given as follows:

$$P = \frac{3}{2} V i_d \tag{38}$$

$$Q = \frac{3}{2} V i_q \tag{39}$$

Therefore, active and reactive power can be controlled by direct and quadrature current components, respectively. The control strategy for grid-side converter is shown as Fig.3. There are two closed-loop controls for the power converter. The fast dynamics are associated with the line

current control in the inner loop where the nonlinear SMC control is adopted to track the line current control. However, in the outer loop slow dynamics is associated with the DC voltage control. In addition, the PI regulator is employed in order to generate the reference source current  $i_{dr-f}$  and regulate the DC voltage, but the reference signal of the q-axis current  $i_{qr-f}$  is produced by the reactive power  $Q_r$  according to (39). Let us introduce the following sliding surfaces:

$$S_{d-f} = i_{dr-f} - i_{d-f} \tag{40}$$

$$S_{q-f} = i_{qr-f} - i_{q-f} \tag{41}$$

where  $i_{qr-f}, i_{dr-f}$  are the desired values of q- axis current and d-axis current respectively. The reference  $i_{qr-f}$  for the  $i_{q-f}$  current is derived from the desired power factor. So:

$$\frac{dS_{d-f}}{dt} = \frac{di_{dr-f}}{dt} - \frac{di_{d-f}}{dt} \tag{42}$$

$$\frac{dS_{q-f}}{dt} = \frac{di_{qr-f}}{dt} - \frac{di_{q-f}}{dt} \tag{43}$$

In permanent regime and during the sliding mode:

$$\frac{dS_{d-f}}{dt} = 0 \tag{44}$$

$$\frac{dS_{q-f}}{dt} = 0 \tag{45}$$

Therefore, the control voltages of q axis and d axis are defined as follows:

$$v_{dr-f} = L_f \frac{di_{dr-f}}{dt} + R_f i_{d-f} - L_f \omega i_{q-f} + V + k_{d-f} \operatorname{sgn}(S_{d-f}) \tag{46}$$

$$v_{qr-f} = R_f i_{q-f} + L_f \omega i_{d-f} + k_{q-f} \operatorname{sgn}(S_{q-f}) \tag{47}$$

Finally, PWM is used in order to produce the control signal. The structure of the DC-link voltage and current controllers for grid-side converter is shown in Fig.3.

### 4. Simulation Results

The system is built using Matlab/Simulink. This paragraph presents the simulated responses of the WECS under variable wind speeds. The parameters of PMSG used are given in Table 1. Fig. 4, Fig. 5 and Fig. 6 show the waveforms of wind speed, rated wind speed, tip speed ratio, pitch angle and power coefficient. Fig. 7 and Fig. 8 show active power, rotor angular velocity and optimum rotor speed.

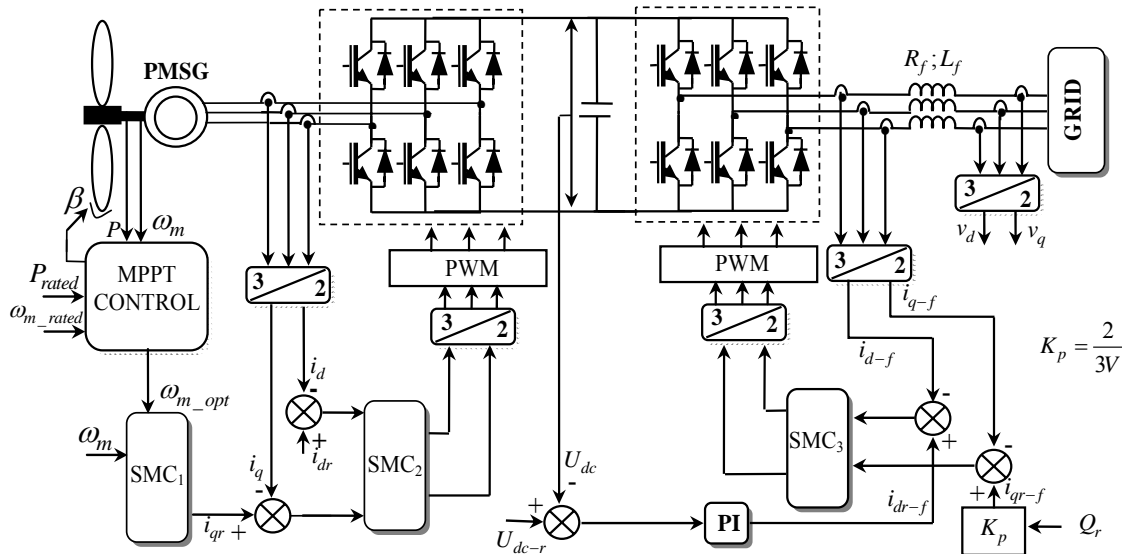


Fig.3. Schematic of control strategy for WECS.

It can be seen that if the wind speed increases, the rotor angular velocity increases proportionally too. Besides, the power coefficient will drop to maintain the rated speed generator. The WECS operate under MPPT control. The initial pitch angle  $\beta$  keeps the value of  $0^\circ$ , the tip speed ratio  $\lambda$  maintains the optimal value 8.1, and

the power coefficient  $C_p$  is the maximum around 0.41. Although, when the wind speed is up the rated wind speed (11.5m/s), the operation of the pitch angle control is actuated and the pitch angle  $\beta$  is increased which has for consequence decreasing power coefficient  $C_p$  and also

the tip speed ratio. Therefore, rotational speed is keeping constant.

Fig. 9 shows the simulation result of DC link voltage that remains a constant value. Fig. 10 shows the variation and a closer observation of three phase current and voltage of grid. The frequency imposed by the grid is 50 Hz. It is obvious that unity power factor is achieved approximatively. Thus, the effectiveness of the established regulators is demonstrated.

Table 1. Parameters of the Power Synchronous Generator

Parameter	Value
$P_r$ rated power	14(kW)
$\omega_m$ rated mechanical speed	25 (rd/s)
$R$ stator resistance	1.764( $\Omega$ )
$L_q$ stator q-axis inductance	0.00448 (H)
$L_d$ stator d-axis inductance	0.00448 (H)
$p_n$ pole pairs	36

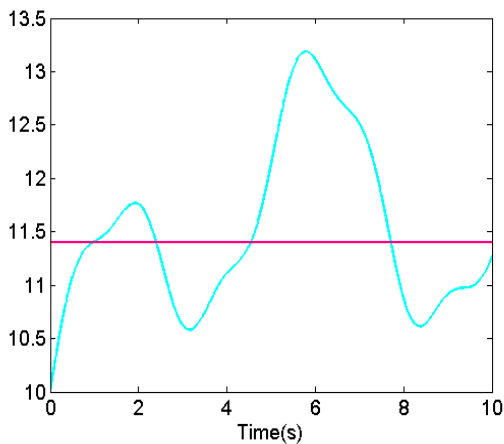


Fig.4. Instantaneous wind speed (m/s) and rated wind speed.

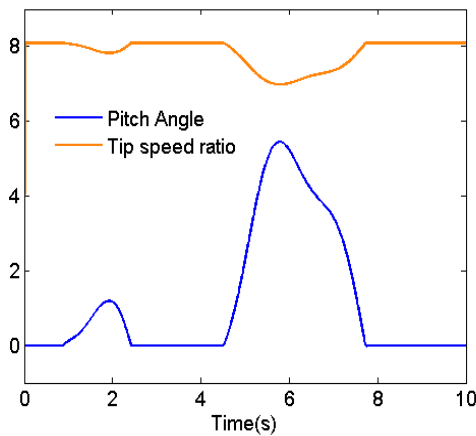


Fig.5. Pitch angle  $\beta$  (in degree) and tip speed ratio  $\lambda$ .

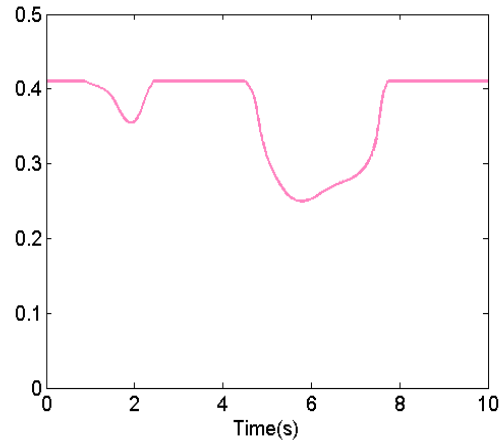


Fig.6 Variation of coefficient power conversion  $C_p$

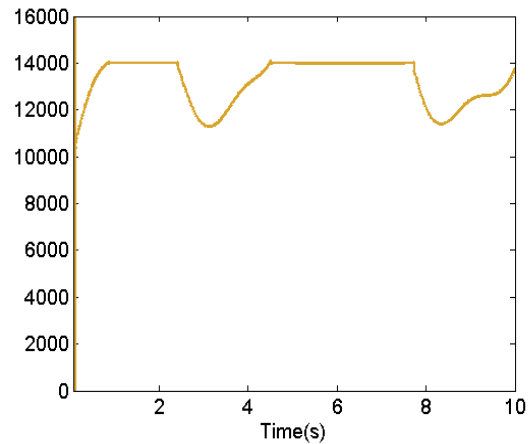


Fig. 7. Power generated (W).

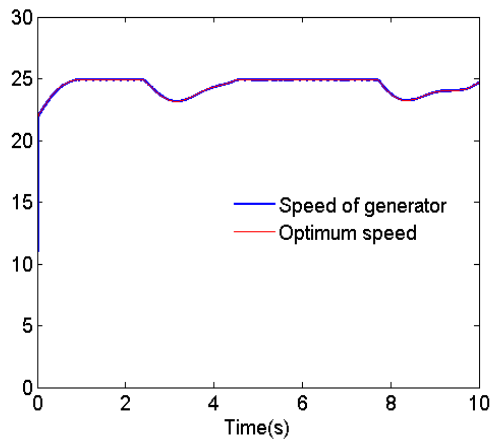


Fig. 8. Speed of PMSG (rd/s)

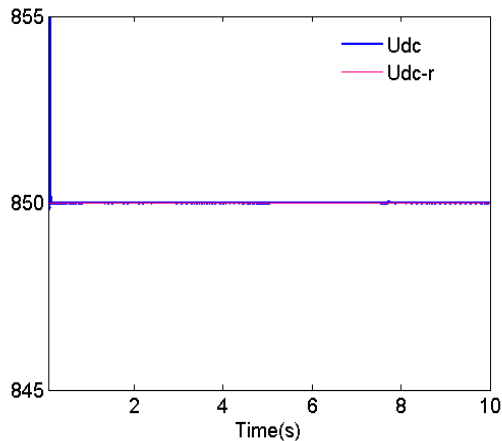
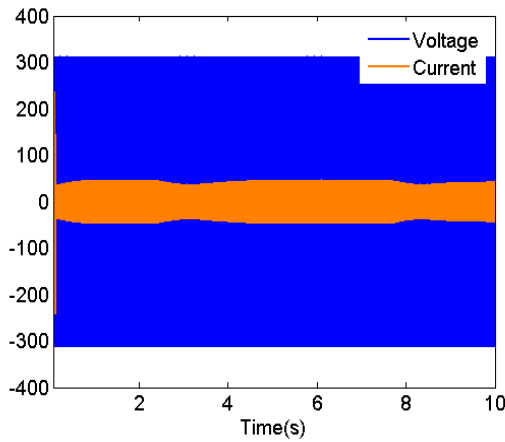
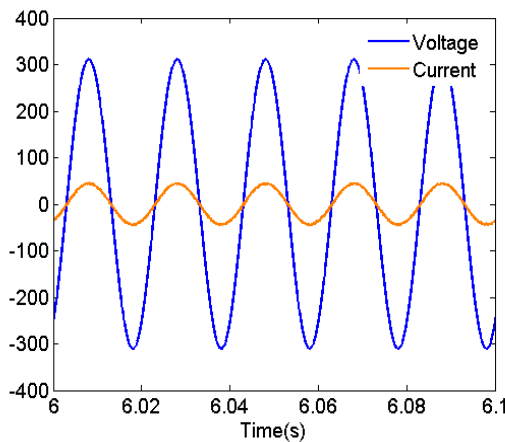


Fig. 9. DC link voltage (V).



(a)



(b)

Fig. 10. The waveforms of three phase current (A) and voltage (V) of grid.

## 5. Conclusions

The sliding mode power control of PMSG for wind generation system has been proposed in this paper. The concept of the MPPT has been presented in terms of the adjustment of the generator rotor speed according to instantaneous wind speed. As the voltage and frequency of generator output vary along the wind speed change, the generator-side converter is used to track the maximum wind power and implement sliding mode control for PMSG. Inverter is used to sustain the DC-bus voltage and regulate the grid-side power factor. Both converters use the sliding mode scheme. The conditions for the existence of the sliding mode are found by using the stability conditions of Lyapunov. Thus, active and reactive powers are controlled respectively by the inverter in grid-side. Simulation results have shown the effectiveness of the proposed control strategy for WECS based on the PMSG.

## References

- [1] Shao Zhang, King-Jet Tseng, D. Mahinda Vilathgamuwa, Trong Duy Nguyen, Xiao-Yu Wang, IEEE Transactions On Industrial Electronics, **58**(1), **316** (2011).
- [2] Chen Jinmei, Xue Ancheng, Tian Chunguang, Bi Tianshu, Gao Changzheng, Proceedings of the 30th Chinese Control Conference, IEEE- Control Conference (CCC), 2011, p. 5114 – 5119.
- [3] Li Shuhui, T.A Haskew, R.P. Swatloski, W. Gathings, IEEE Transactions on Power Electronics, **27**(5), 2325 (2012).
- [4] Y.Xia, K.H Ahmed, B.W. Williams, IEEE Transactions on Power Electronics, **26**(12), 3609 (2011).
- [5] K.H. Kim, Y.C. Jeung, D.C. Lee, H.G. Kim, IEEE Transactions On Power Electronics, **27**(5), 2376 (2012).
- [6] Md. Enamul Haque, Michael Negnevitsky, Kashem M. Muttaqi, IEEE Transactions On Industry Applications, **46**(1), 331 (2010).
- [7] F. Blaabjerg, F. Iov, Z. Chen, K. Ma, IEEE-Energy Conference and Exhibition (EnergyCon), pp. 333 – 344, December 2010.
- [8] Zhe Chen, Josep M. Guerrero, Frede Blaabjerg, IEEE Transactions on power electronics, **24**(8), 1859 (2009).
- [9] Jiacheng Wang, Dewei (David) Xu, BinWu, Zhenhan Luo, IEEE Transactions On Power Electronics, **26**(8), 2192 (2011).
- [10] Mingxing Zhou, Guangqing Bao, Youmin Gong, Proceeding of IEEE-Power and Energy Engineering Conference (APPEEC), Asia-Pacific, pp. 1 – 4, March 2011.
- [11] S. M. Muyeen, Rion Takahashi, Junji Tamura, IEEE Transactions On Sustainable Energy, **1**(1), 30 (2010).

- [12] A. Mesemanolis, C. Mademlis, I. Kioskeridis, Proceedings of 7th IEEE Mediterranean Conference and Exhibition on Power Generation, Transmission, Distribution and Energy Conversion (IEEE-MedPower), pp. 1-9, November 2010.
- [13] Li Shuhui, T. A Haskew, R. P. Swatloski, W. Gathings, IEEE Transactions on Power Electronics, **27**(5), 2325 (2012).
- [14] V. I. Utkin, IEEE Transactions on Automatic Control, **22**(2), 212 (1977).
- [15] D. Kairous, R. Wamkeue, Bachir Belmadani, 9th IEEE International Conference on Environment and Electrical Engineering (EEEIC), pp. 41, Mai 2010.
- [16] S. Wen, F. Wang, Proceedings of International conference on Electrical Machines and Systems ICEMS-IEEE, pp. 995, October 2008.

---

\*Corresponding authors: [errami.emi@gmail.com](mailto:errami.emi@gmail.com),  
[ouassaid@emi.ac.ma](mailto:ouassaid@emi.ac.ma)